0 0 0 0 4 5 0 1 9 2 6

Lectures delivered at Les Houches Summer
School, Les Houches, France,
June 3 - 28, 1975

LBL-4811
c.1

MANY-PARTICLE DISPERSION RELATIONS

Henry P. Stapp

RECEIVED
LAWRENCE
RADIATION LABORATORY

MAR 24 1978

LIBRARY AND
DOCUMENTS SECTION

March 1976

Prepared for the U. S. Energy Research and
Development Administration under Contract W-7405-ENG-48

For Reference

Not to be taken from this room

LAWRENCE BERKELEY LABORATORY
UNIVERSITY OF CALIFORNIA
BERKELEY

LBL-4811
c.1

DISCLAIMER

This document was prepared as an account of work sponsored by the United States Government. While this document is believed to contain correct information, neither the United States Government nor any agency thereof, nor the Regents of the University of California, nor any of their employees, makes any warranty, express or implied, or assumes any legal responsibility for the accuracy, completeness, or usefulness of any information, apparatus, product, or process disclosed, or represents that its use would not infringe privately owned rights. Reference herein to any specific commercial product, process, or service by its trade name, trademark, manufacturer, or otherwise, does not necessarily constitute or imply its endorsement, recommendation, or favoring by the United States Government or any agency thereof, or the Regents of the University of California. The views and opinions of authors expressed herein do not necessarily state or reflect those of the United States Government or any agency thereof or the Regents of the University of California.

0 0 0 0 4 5 0 1 9 2 7

MANY-PARTICLE DISPERSION RELATIONS*

Henry P. Stapp

Lawrence Berkeley Laboratory
University of California
Berkeley, California 94720

This lecture describes work done in collaboration with Alan White on the analytic foundations of Regge theory. The work ties together the analyticity results described in the previous lectures with White's results on Regge theory. The study is very recent and not yet complete. But the beautiful way everything hangs together to give exactly what is needed for a systematic derivation of Regge theory encourages us to describe here what we have done and what we expect to be able to do. First I shall describe the parts that are closely tied to the results on direct channel unitarity described in my earlier lectures. Then White will carry on.

1. Toller Variables

The first main idea is to disperse in the Toller boost variables keeping the Toller momentum transfer and helicity variables fixed. The Toller variables are described in Ref. (1). I shall give here only a brief resume.

For any n-particle scattering function there are many possible sets of Toller variables. We shall use each of these sets. Each set of Toller variables is associated with a planar Toller diagram, which is a planar tree diagram with n external lines (one for each of the n particles) and $n-3$ internal lines. Precisely three lines meet at each vertex. Some examples of Toller diagrams for the case $n = 6$ are shown in Fig. 1. (I discuss only the case where all external particles are spinless.)

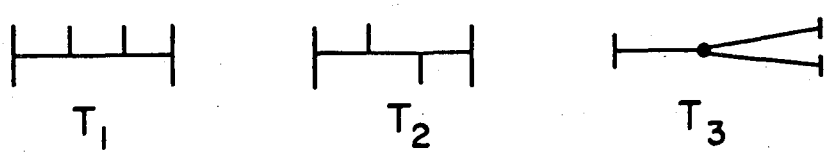

Fig. 1. Some Toller diagrams for $n = 6$.

Each internal and external line i is assigned a conventional direction, and the momentum-energy flowing along the line in that direction is defined to be p_i. For each of the $n-3$ internal lines i this vector is also called Q_i, and the $n-3$ invariants

*This work was supported by the U.S. Energy Research and Development Administration.

$$t_i = Q_i^2 \tag{1.1}$$

are called the <u>momentum transfer variables</u> associated with the Toller diagram.

The <u>direct channel</u> (or s channel) is the region where energy flows upward in the Toller diagram. Initially we consider a part of the direct channel where all t_i are negative.

The remaining variables associated with the Toller diagram are defined by associating with each ordered pair (i,v), consisting of a line i of the diagram and a vertex v touched by i, a standard frame $\sum_{iv}$. In this frame the vector p_i has a standard form p_{io}, which is either $(m_1,0,0,0)$ or $(0,0,0,\sqrt{-t_i})$.

The various frames can be represented by dots on the Toller diagram, as in Fig. 2

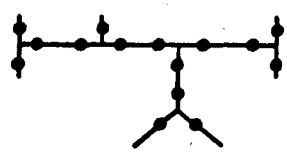

Fig. 2. The standard frame $\sum_{iv}$ is represented by a dot on line i near vertex v.

The Lorentz transformation that takes components from their values in $\sum_{iv}$ to their values in $\sum_{jv}$ is called ζ_{ji}. The Lorentz transformation that takes components from their values in $\sum_{iv}$ to their values in $\sum_{iw}$ (where line i points from v to w) is called g_i. Thus the components of p_i in frame $\sum_{jv}$ are given by

$$p_i^{(j,v)} = \zeta_{jn} g_n \cdots \zeta_{m\ell} g_\ell \zeta_{\ell k} g_k \zeta_{ki} p_{io} \quad , \tag{1.2}$$

provided a path in T from i to j runs along the sequence of lines $k,\ell,m,\cdots,n$, moving in the positive direction along each of these lines. If the direction of some intermediate line is reversed then the corresponding g is replaced by g^{-1}.

The standard frames are chosen so that g_i is specified by a single boost angle β_i. Let k be the third line that meets i and j. If either i or j is external then ζ_{ij} is completely determined by the masses (m's and t's) of the three lines i, j, and k. If both i and j are internal then ζ_{ij} depends on an helicity angle ω_{ij}. If i, j, and k are all internal then the constraint

$$\omega_{ij} + \omega_{jk} + \omega_{ki} = 0$$

holds. Thus for each Toller diagram there are (n-3) momentum transfer variables t_i, (n-3) boost angles β_i, and (n-4) independent helicity angles ω_{ij}, for a total of 3n-10. A scattering function f written as a function of the Toller variables $t_i, v_i = \exp \beta_i$, and $u_{ij} = \exp i\,\omega_{ij}$ corresponding to Toller diagram T will be called the Toller function f^T.

The expressions for the invariants in terms of the Toller variables are generally quite complicated. However, the square of the momentum-energy flowing across (t ansverse to) any internal line i is given by a simple formula

$$s_i = f_i + g_i \cosh \beta_i \equiv f_i + g_i z_i \tag{1.3}$$

where f_i and g_i depend only on the t's (and masses m). Moreover, if two lines a and b are linked by a sequence of internal lines ijk···n then, for large β_i, one may use the formula

$$p_a \cdot p_b = m_{ai}\, z_i\, w_{ij}\, z_j\, w_{jk} \cdots w_{mn}\, z_n\, m_{nb} + r_{ab} \quad , \tag{1.4a}$$

where the remainder r_{ab} has at least one less factor z_λ. For any internal line i

$$z_i = \cosh \beta_i = \frac{1}{2}(v_i + v_i^{-1}) \quad . \tag{1.4b}$$

For any pair of touching internal lines i and j

$$w_{ij} = (\cos \omega_{ij} + \cosh \xi_{ij}) \quad , \tag{1.4c}$$

where

$$\sinh \xi_{ij} = \left(\lambda(p_i^2, p_j^2, p_k^2)/4t_i t_j\right)^{\frac{1}{2}} \quad . \tag{1.4d}$$

For any pair of touching lines a and i, where i is internal,

$$m_{ai} = \left(\lambda(p_a^2, p_i^2, p_k^2)/-4t_i\right)^{\frac{1}{2}} \tag{1.4e}$$

where

$$\lambda(a,b,c) = a^2 + b^2 + c^2 - 2ab - 2bc - 2ac \quad . \tag{1.4f}$$

The line k is the third line at vertex (ijk) or (iak). The formula holds in the portion of the direct-channel region where all the t_i are negative and all the λ's are positive, provided lines a and b are both external and directed upward. It also holds if b is external and directed upward and a is internal and directed upward--in the frame where line i is horizontal. (The internal lines are regarded as almost horizontal but making an angle of $90^\circ+\varepsilon$ with any external line they touch, and an angle of $180^\circ-2\varepsilon$ or 4ε with any internal line they touch. Here ε is very small but positive.)

2. Bergman-Weil Representation

The dispersion relation we use, like the Mandelstam representation, is a special case of the Bergman-Weil representation. (Fronsdal (2), Fuks (3), Stapp (4).)

Let $z \equiv (z_1,\cdots,z_N)$ be any set of N complex variables. Let $F(z)$ be a function that is holomorphic in the region

$$R \equiv \{z\colon \operatorname{Im} Z_c(z) > 0 \qquad \text{all } c \in C\}, \tag{2.1}$$

where C is some finite index set, and the functions $Z_c(z)$ are entire functions. Let Γ_λ denote a subset of N of the variables $c \in C$, and let

$$Z^\lambda \equiv \{Z_1^\lambda, Z_2^\lambda, \cdots, Z_N^\lambda\} \tag{2.2}$$

be the N variables Z_c for $c \in \Gamma_\lambda$. Let $J_\lambda(z)$ be the Jacobian

$$J_\lambda(z) \equiv \left| \frac{\partial Z_i^\lambda(z)}{\partial z_j} \right| \geqslant 0 \ . \tag{2.3}$$

Define the region

$$I_\lambda \equiv \{z \in \bar{R}\colon \operatorname{Im} Z_i^\lambda = 0 \quad \text{for } i = 1,\cdots,N, \text{ and } J_\lambda(z) \neq 0\} \ . \tag{2.4}$$

Consider the mapping $X^\lambda(z)$ from I^λ into Z^λ space: i.e., for any point $z \in I_\lambda$ let

$$X^\lambda(z) \equiv \left(X_1^\lambda(z),\cdots,X_N^\lambda(z)\right) \tag{2.5}$$

be the set of N real numbers

$$X_i^\lambda(z) = \operatorname{Re} Z_i^\lambda(z) \ . \tag{2.6}$$

Several different points $z \in I_\lambda$ may map onto the same point X^λ. Let

$$z_\alpha^\lambda(X^\lambda) \in I_\lambda \tag{2.7}$$

for $\alpha = 1,\cdots,$ be the various points z in I_λ that map to the point X^λ. The Bergman-Weil formula implies that for each pair (λ,α) there is a kernel function $K_\alpha^\lambda(Z^\lambda,z)$ (which is holomorphic in Z^λ and z for Z^λ in $Z^\lambda(I^\lambda)$ and z in $\mathbb{C}^N$) such that the function $\hat{F}(z)$ defined by

$$\hat{F}(z) = \sum_{\lambda,\alpha} \left[\frac{1}{(2\pi i)^N} \int_{X^\lambda(I_\lambda)} \cdots \int dX_1^\lambda \cdots dX_N^\lambda \, K_\alpha^\lambda(X^\lambda,z) \right.$$

$$\left. \times \, F\left(z_\alpha^\lambda(X_1^\lambda + io,\cdots,X_N^\lambda + io)\right) \frac{1}{X_1^\lambda - Z_1^\lambda(z)} \cdots \frac{1}{X_N^\lambda - Z_N^\lambda(z)} \right] \tag{6.8a}$$

satisfies

$$\begin{aligned} \hat{F}(z) &= F(z) \qquad \text{for } z \text{ inside } R \\ \hat{F}(z) &= 0 \qquad \text{for } z \text{ outside } \bar{R} \ , \end{aligned} \tag{2.8b}$$

where $\bar{R}$ is the closure of R.

MANY-PARTICLE DISPERSION RELATIONS

The kernel function $K_\alpha^\lambda(X^\lambda,z)$ has the important property

$$K_\alpha^\lambda\left(X^\lambda, z_\beta^\lambda(X^\lambda)\right) = \delta_{\alpha\beta} \quad . \tag{2.9}$$

That is, $K_\alpha^\lambda(X^\lambda,z)$ is unity if $z = z_\alpha^\lambda(X^\lambda)$, but is zero if $z = z_\beta^\lambda(X^\lambda)$ for any $\beta \neq \alpha$. This property of K_α^λ effects a separation of the contributions from the different points z_α that correspond to a single point X^λ in the integration domain $X^\lambda(I^\lambda)$.

Consider a function $F(z)$ that is holomorphic in a region R except for cuts confined to the surfaces $\mathrm{Im}\, Z_c(z) = 0$ for $c \in C$. These cuts separate R into a set of regions $R_1, R_2, \cdots$. (See Fig. 3.)

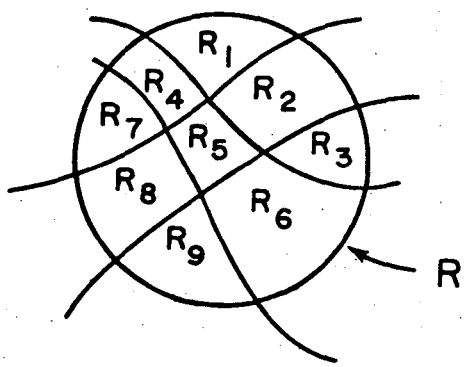

Fig. 3. The region R in z space is separated into regions $R_1, \cdots R_9$ by the surfaces $\mathrm{Im}\, Z_c(z) = 0$.

By simply adding the formulas (2.8) corresponding to the different regions R_i one obtains a formula for $F(z)$ valid in the union of the R_i.

In this composite formula there will generally be several different contributions from each region I_λ. These are the contributions from the boundary values from the different combinations of sides of the cuts that pass through I. These contributions can be lumped together. Suppose no two regions I_λ coincide unless they are defined by the same set of N equations $\mathrm{Im}\, Z_i^\lambda = 0$. That is, suppose the different regions R_i that give contributions from a fixed integration region I_λ are just the 2^N regions corresponding to the different possible combinations of sides of the N cuts $\mathrm{Im}\, Z_i^\lambda = 0$ that define I^λ. Then the full contribution from I_λ is obtained by replacing the function $F\left(z_\alpha^\lambda(X_1^\lambda + io, \cdots, X_N^\lambda + io)\right)$ in (2.8) by the N-fold multiple discontinuity

$$\Delta\left(z_\alpha^\lambda(X^\lambda)\right) = \sum (-1)^n F\left(z_\alpha^\lambda(X_1^\lambda \pm io, X_2^\lambda \pm io, \cdots, X_N^\lambda \pm io)\right) \quad . \tag{2.10}$$

Here the $\pm io$ indicate the appropriate boundary value, the sum is over the 2^N possible boundary values, and n is the number of arguments $(X_i^{\lambda} - io)$.

If the regions I_λ defined by several different sets of N surfaces coincide over an N dimensional region then one must consider a tiny displacement of some of these surfaces away from the degenerate-case location.

Equations (2.8) and (2.10) yield a suitable generalization of the Mandelstam representation. However, we will disperse only in the $n-3$ boost variables v_i (or z_i), not in a full set of $3n-10$ variables. Thus we are dealing with a multi-variable generalization of the <u>fixed-t</u> dispersion relations of earlier works on $2 \to 2$ scattering amplitudes.

3. Accessible Boundaries

Let the Toller functions f^T be regarded as functions of the $(n-3)$ complex variables v_i (or z_i) with the t_i and w_{ij} held fixed and real. In this space of $n-3$ variables (which we shall call the z_i's) we shall apply the Bergman-Weil formulas (2.8) and (2.10) of the preceding section. The contributions from the intersections I_λ of $N = n-3$ of the normal threshold cuts $\mathrm{Im}\, s(c) = \mathrm{Im}\, Z_c(z) = 0$ are considered first.

Note first that each of these regions I_λ contains the whole physical region, which is a certain portion of the $n-3$ dimensional space $x = \mathrm{Re}\, z$ space. Thus to use (2.8) and (2.10) we must slightly displace some of the cuts $\mathrm{Im}\, s(c) = 0$, in order to shift the various regions I_λ away from each other. This is illustrated in Fig. 4, for the case $N = 2$.

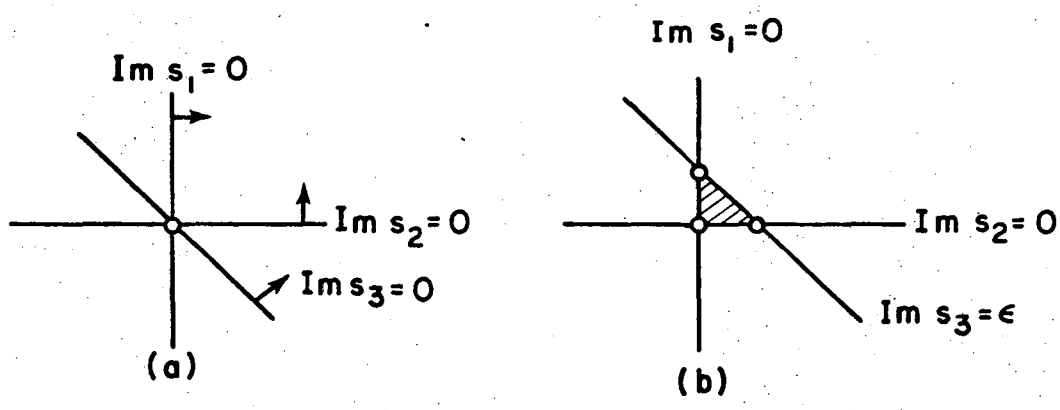

Fig. 4. All three cuts $\mathrm{Im}\, s_i = 0$ intersect on one $N = 2$ dimensional region, represented by the dot in (a). A slight shift of one cut separates this intersection region into three separate regions I_λ each involving only $N = 2$ cuts. Now (2.8) and (2.10) can be applied.

MANY-PARTICLE DISPERSION RELATIONS

The first important point is that the shaded region is introduced artifically and disappears in the limit $\varepsilon \to 0$. Because we are basically concerned here only with the function in the various outer unshaded regions we can define the function in the shaded region in any convenient manner. For example, we could define it to be zero. Or we could define it differently in different regions separated by a sequence of cuts $\mathrm{Re}\ \phi_j(z) = 0$, as indicated in Fig. 5.

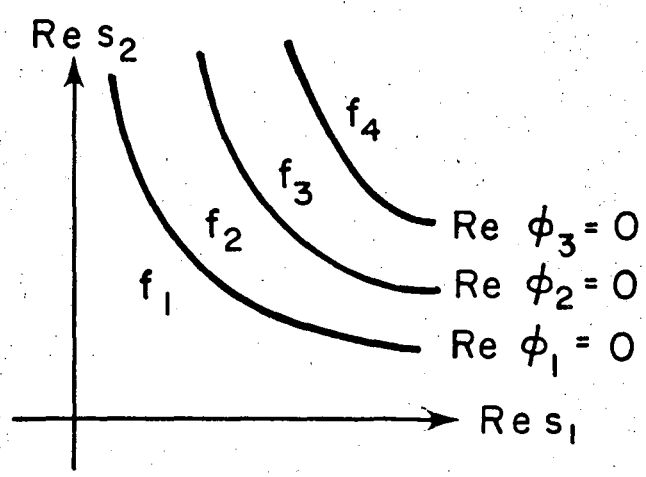

Fig. 5. The function in the tiny shaded region of Fig. 4b can be defined to be different analytic functions in the regions separated by surfaces $\mathrm{Re}\ \phi_j(z) = 0$.

Of course there will be contributions to the Bergman-Weil formula associated with the surfaces $\mathrm{Re}\ \phi_j(z) = 0$ where the definition of the function changes. But the integration is only over the tiny intersection of the boundary of the shaded region with the surface $\mathrm{Re}\ \phi_j(z) = 0$. Thus its effect outside the shaded region drops away as $\varepsilon \to 0$. The introduction of functions corresponding to the shaded regions defined by combinations of more than N cuts is clearly just an artifice that allows the N-fold multiple discontinuity functions to be used.

The restriction to the space of just $n-3$ complex variables, with the t_i and w_{ij} kept real, induces relations between the imaginary parts of the variables $s(c) = Z_c(z)$. For example, if the variables of Fig. 4a increase in the directions indicated by the arrows then the boundary from the region $\mathrm{Im}\ s_1 > 0$, $\mathrm{Im}\ s_2 > 0$, $\mathrm{Im}\ s_3 < 0$ is not accessible. In general the inaccessible boundaries are boundaries accessible only if some of the cuts are infinitesimally displaced to expose an infinitesimal region analogous to the shaded region of Fig. 4b.

Asymptotically, for the six-particle case, the accessible boundaries are all good functions M^G, in the terminology of the previous lectures. That is, the bad boundaries, which correspond to functions that are not single analytic functions are always inaccessible, asymptotically. Hence we are free, at least asymptotically, to define the inaccessible boundary values to be just the corresponding functions M^G.

Taking the inaccessible boundary values to be the functions M^G leads to many important simplifications:

(1) The formula becomes independent of the sign of ε occurring in Fig. 4b. This awkward dependence disappears because the generalized Steinmann relations entail that the $(n-3)$ fold discontinuities do not depend on upon which sides of the remaining cuts they are evaluated.

(2) All of the $n-3$ fold multiple discontinuities are given by simple known bubble diagram functions. Thus one has a well-defined basis for the study of the question of whether any complex singularities extrude into the complex plane.

(3) The generalized Steinmann relations reduce the number of spectral terms: The multiple-discontinuity Δ_α^λ vanishes if the set Γ_λ of $n-3$ cuts contains any pair corresponding to overlapping channels.

(4) The generalized Steinmann relations allow a unique correspondence to be established between hexagraphs and specified sets of Bergman-Weil components. (See below.) It is this hexagraphical decomposition of the Toller functions into well-defined hexagraphical components with specified analytic properties that is the basis of White's analysis.

4. Hexagraphs

A decisive new step is a decomposition of each Toller function f^T into sum of components. There is one component for each way that the Toller diagram T can be drawn as a hexagraph.

A hexagraph is a planar tree diagram such that each vertex is drawn as a meeting of one horizontal line and two sloped lines, with the angle between each pair emerging rays approximately 120°. The external lines must be sloped and in the direct channel energy flows upward along these external lines. Each internal line of the Toller diagram is mapped into a horizontal segment of the corresponding hexagraph, as is shown in Fig. 6.

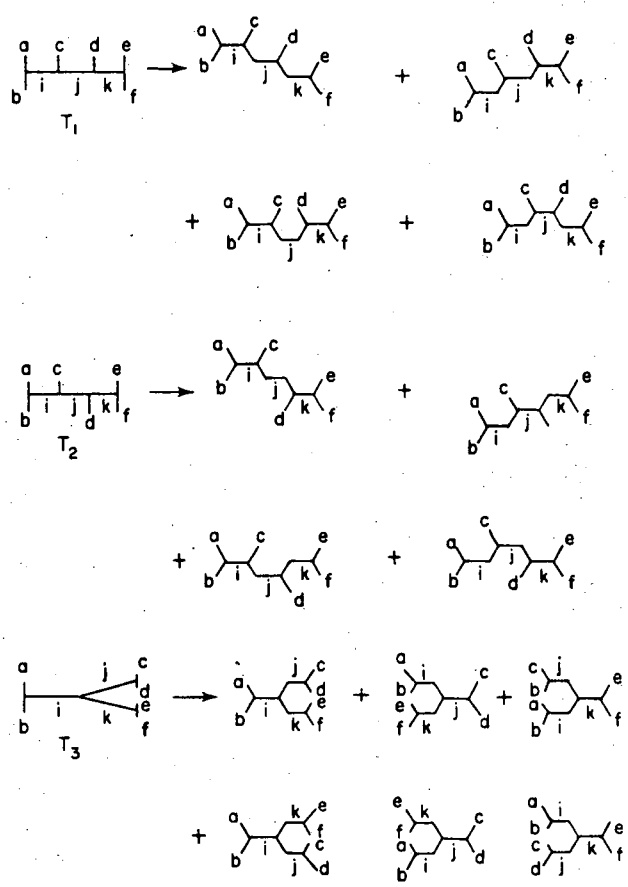

Fig. 6. The hexagraphs for Toller diagrams T_1, T_2, and T_3.

5. Flow Graphs

Flow graphs are graphs that represent the flow of energy in the direct channel, as will be explained later. Each hexagraph maps into a unique flow graph. This graph is constructed by replacing each vertex of the hexagraph by a set of flow lines according to the rules of Fig. 7.

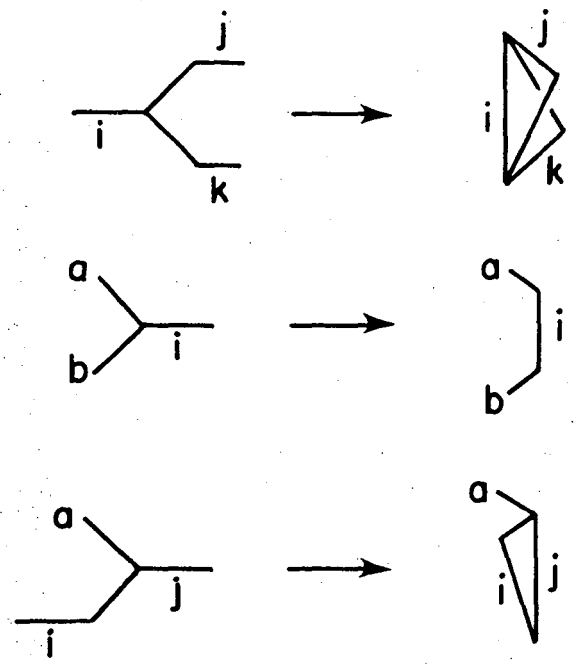

Fig. 7. The rules for converting a hexagraph to a flow graph. Lines i, j, and k are internal lines. Lines a and b are external lines.

The flow graphs corresponding to the Toller diagrams T_1, T_2, and T_3 are shown in Figs. 8, 9, and 10, respectively.

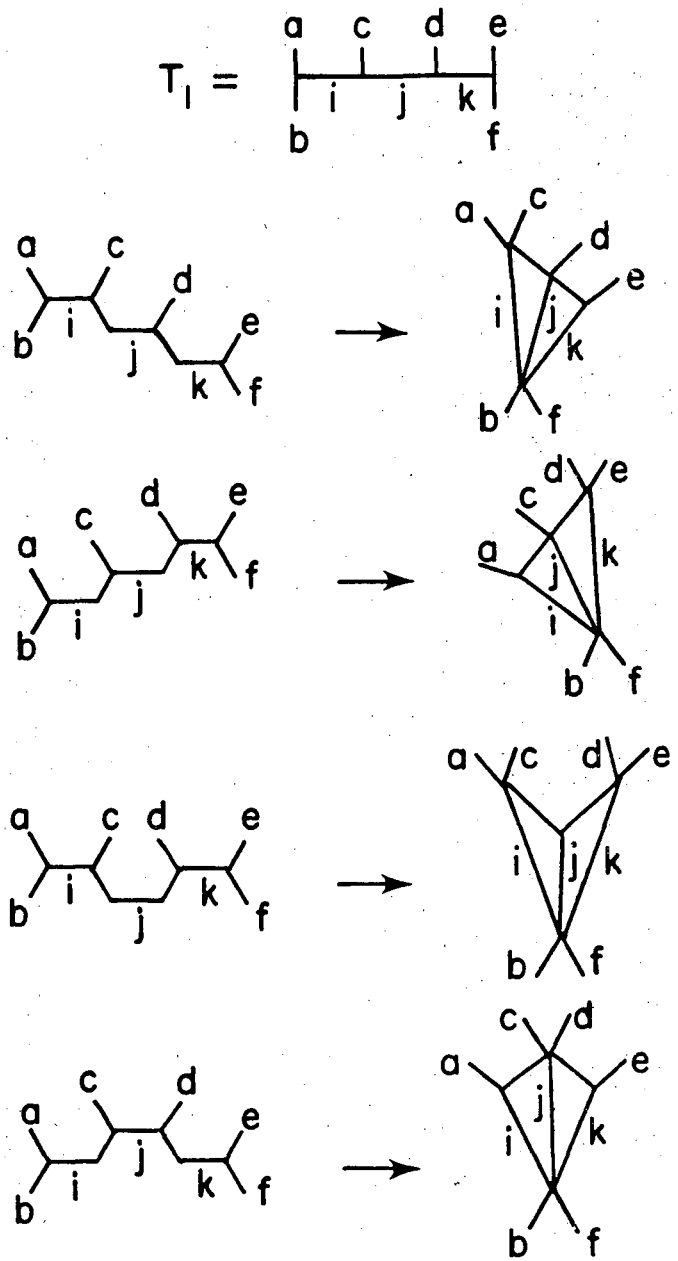

Fig. 8. The basic flow graphs corresponding to the Toller diagram T_1.

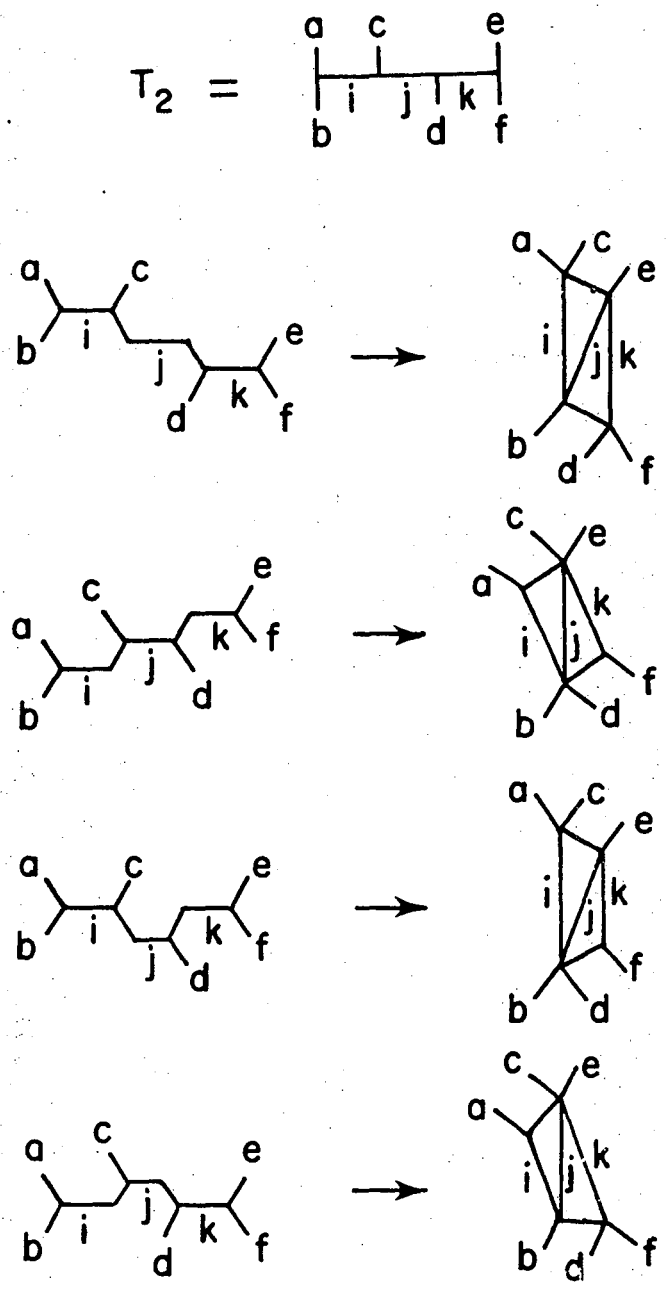

Fig. 9. The basic flow graphs corresponding to the Toller diagram T_2.

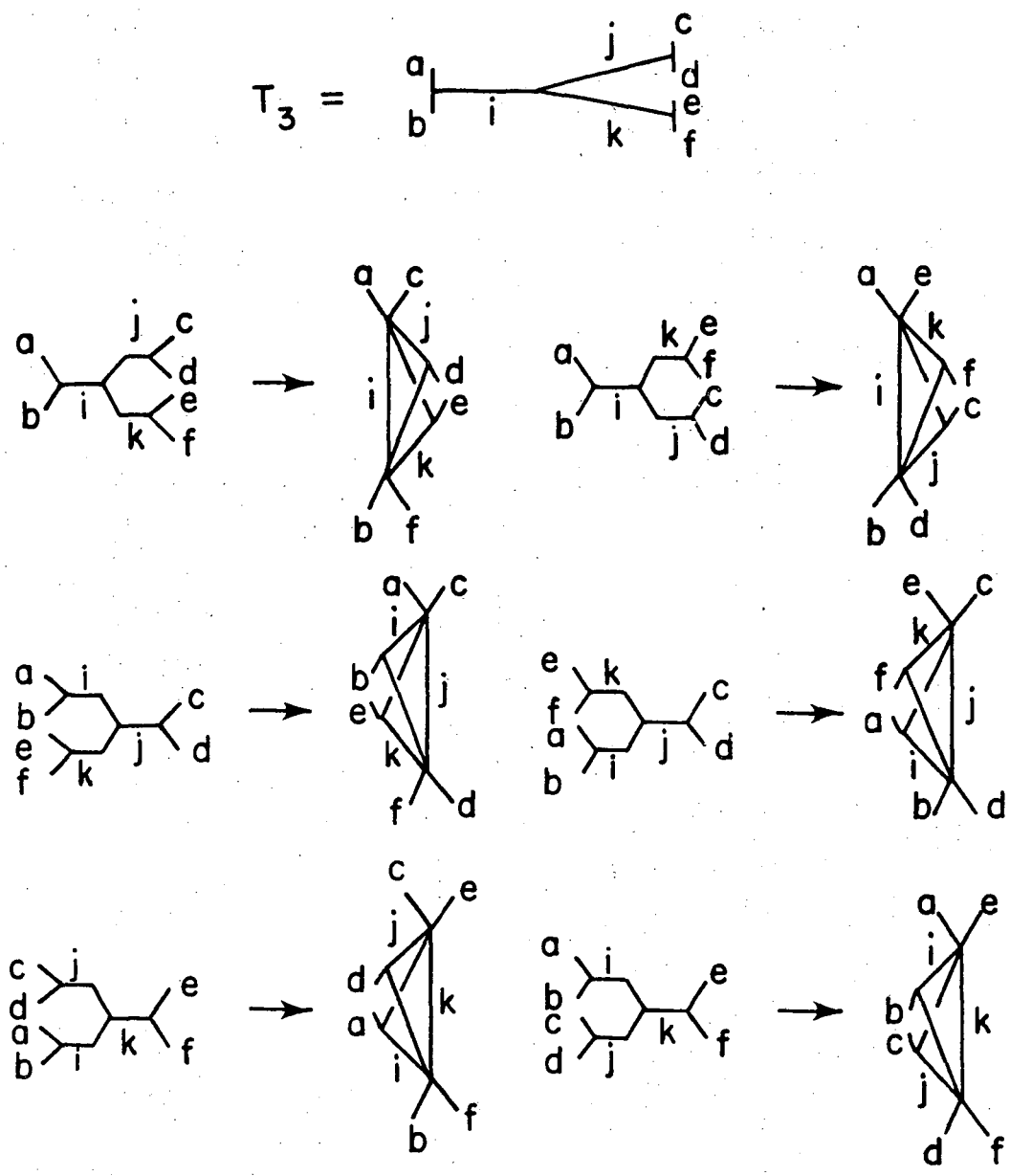

Fig. 10. The basic flow graphs corresponding to the Toller diagram T_3.

The flow graphs shown in Figs. 8, 9, and 10 are the basic, or uncontracted, flow graphs corresponding to the Toller diagram in question. We shall also use the graphs obtained from these by the contraction of one or more internal lines. Flow graphs are reduced to skeleton graphs by removing extra lines.

Energy-momentum is considered to flow upward along each line of a flow graph. Then for each flow graph F there is a unique set C^F of normal-threshold cuts c:

$$C^F \equiv \{c\text{: } F \text{ contracts to } D_c\} \quad . \tag{5.1}$$

Here D_c is the diagram corresponding to the normal-threshold cut c (see Fig. 11).

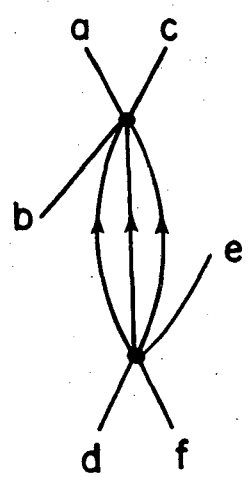

Fig. 11. The diagram D_c corresponding to the normal-threshold cut $c = (abc)$ or $\bar{c} = (def)$.

A diagram corresponding to a normal threshold cut has exactly two vertices, one initial and one final, and energy flows from the initial vertex to the final vertex along every internal line.

The cut c associated with the diagram D_c shown in Fig. 11 is a cut that lies along the positive real axis of the variable

$$s(c) = (p_a + p_c - p_b)^2 = (p_e - p_d - p_f)^2 .$$

Let $\hat{T}$ be the set of basic flow graphs constructed from the planar Toller diagram T according to the rules described above. Then

$$C^T \equiv \bigcup_{F \in \hat{T}} C^F \tag{5.2}$$

0 0 0 0 4 5 0 1 9 3 4

is a set of normal threshold cuts associated with the planar Toller diagram T.

6. Theorems on Hexagraphs

The importance of hexagraphs rests on some properties summarized in theorems described in this section. Some definitions will first be introduced.

A lower case c will represent one of the normal threshold cuts. An upper case C will represent a set of cuts c. And a script $\mathcal{C}$ will represent collections of sets C. The symbol $\tilde{H}$ will represent an equivalence class of hexagraphs connected to each other by twists about horizontal lines. For example

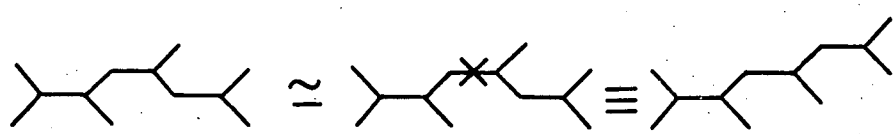

where $\simeq$ denotes equivalence. Similarly, $\tilde{T}$ denotes an equivalence class of planar Toller diagrams.

Introduce now

$$C(\tilde{H}) \equiv \{c: c \in C^{F(H)} \quad \text{for some } H \in \tilde{H}\} \tag{6.1}$$

$$(\tilde{H}) \equiv \{C: C \subset C(\tilde{H})\} \tag{6.2}$$

$$\begin{aligned} C(\tilde{T}) &\equiv \{c: c \in C^{T} \quad \text{for some } T \in \tilde{T}\} \\ &\equiv \{c: c \text{ is not a momentum transfer variable } t_i \text{ of } \tilde{T}\} \end{aligned} \tag{6.3}$$

$$(\tilde{T}) \equiv \{C: C \subset C(\tilde{T}) \text{ is a set of } n-3 \text{ asymptotically distinct cuts in nonoverlapping channels}\} \ . \tag{6.4}$$

Asymptotically distinct cuts are cuts that do not have the same leading term as all $z_i \to \infty$. A set of nonoverlapping channels is a set of channels no pair of which overlap. (A pair of channels overlap if and only if each of the two sets of indices that define one channel intersect each of the two sets that define the other.) A set of $n-3$ nonoverlapping channels can be represented by a tree diagram τ having only 3-line vertices. Introduce also

$$\mathcal{H}(\tilde{T}) \equiv \{\tilde{H}: H \text{ has the topological structure } \tilde{T}\}. \tag{6.5}$$

<u>Theorem A</u> For each linear $\tilde{T}$ and each $C \in \mathcal{C}(\tilde{T})$ there is one and only one $\tilde{H} \in \mathcal{H}(\tilde{T})$ such that

$$C \in \mathcal{C}(\tilde{H}) \ . \tag{6.6}$$

This unique $\tilde{H}$ is denoted by $\tilde{H}(C)$.

This theorem says that each principal contribution to the (multivariable fixed-t) dispersion relation for f^T is associated with a unique hexagraph $\tilde{H}$. A principal contribution is a contribution associated with $n-3$ normal threshold cuts that are asymptotically distinct. (Cuts that are not asymptotically distinct will be treated, asymptotically, as single cuts.) Sets of cuts in channels that are not nonoverlapping give no contribution to the dispersion relations, because of the generalized Steinmann relations.

The correspondence between a principal contribution, defined by a set $C \in \mathcal{C}(\tilde{T})$, and the corresponding $\tilde{H}(C)$ is this: $\tilde{H}(C)$ is the only hexagraph such that each of the cuts c of C is present in $\tilde{H}$, in the sense that some flow graph $F(H)$ with $H \in \tilde{H}$ has this cut c.

This theorem provides a classification of the principal contributions to the dispersion relations into terms corresponding to different hexagraphs $\tilde{H}$. The sum of terms corresponding to any given hexagraph will be called a hexagraphical component. Each hexagraphical component will be treated differently in White's development of Regge theory.

For any flow diagram or skeleton diagram F define

$$\mathcal{C}(F) \equiv \{C\colon C \text{ is a set of cuts } c \in C^F\} \quad . \tag{6.7}$$

<u>Theorem B</u> For any linear $\tilde{T}$, and any flow diagram or skeleton diagram F, every $C \in \mathcal{C}(\tilde{T}) \cap \mathcal{C}(F)$ has the same $\tilde{H}(C)$. (6.8)

This theorem ensures that in the decomposition of f^T into hexagraphical components all parts that correspond to any single flow graph or skeleton graph stay together.

<u>Theorem C</u> Asymptotically, for $n = 6$, the physical sheet near real points p is bounded only by normal threshold cuts: all other singularities and cuts move behind, or onto, the normal threshold cuts as all $z_i \to \infty$.

This theorem has not been proved, but is strongly indicated.

<u>Theorem D</u> For $n = 6$ the boundary values corresponding to bad G's are asymptotically inaccessible.

To see why this is true consider the Toller diagram T_2 of Fig. 9. The only bad boundaries that can be defined using the cuts in C^{T_2} are those associated with the cuts of Fig. 12.

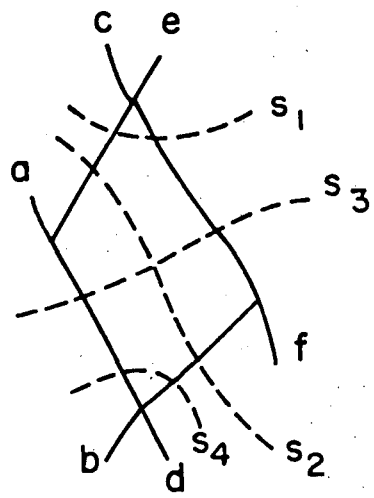

Fig. 12. A flow diagram $F \in \hat{T}_2$, with lines indicating the four associated normal threshold variables s_c, with $c \in C^F$.

The bad boundary is defined by the conditions

$$\text{sign Im } s_1 = -\text{sign Im } s_2 = -\text{sign Im } s_3 = \text{sign Im } s_4 \ . \tag{6.1}$$

However, formula (1.4) gives,

$$s_1 s_4 \sim c s_2 s_3 \tag{6.2}$$

where c is a positive real number. Equations (6.1) and (6.2) are incompatible $\left(\text{for } {}_{T_2}|\text{Im } s_i| \ll \text{Re } s_i \gg 0\right)$. Thus the bad boundaries defined by the cuts $c \in C^2$ are not accessible asymptotically.

Although (6.2) is an asymptotic relation the conclusion is true more generally. The point is that the four s_i's are functions of three variables z_j, and hence there is a constraint between them:

$$\phi(s_1, s_2, s_3, s_4) = 0 \ . \tag{6.3}$$

Equation (6.2) entails that the signs of the components of grad ϕ in the asymptotic limit are these:

$$\text{signs} = \pm(+,-,-,+) \ . \tag{6.4}$$

On the other hand, condition (6.1) says that the signs of the components of

$$\delta(\text{Im } s) = \delta(\text{Im } s_1, \text{Im } s_2, \text{Im } s_3, \text{Im } s_4) \tag{6.3}$$

also satisfy (6.4). Consequently the constraint

$$\delta(\text{Im } s)\cdot\text{grad } \phi = 0 \tag{6.6}$$

cannot be satisfied asymptotically. However, the direction of grad ϕ generally changes in a continuous fashion. Thus the bad boundary will be inaccessible in some neighborhood of infinity: i.e., in the full region where the signs of the components of grad ϕ conform to (6.4).

7. Conclusions

The main conclusion is that in the asymptotic domain the analytic structure greatly simplifies: one probably obtains a simple cut-plane analytic structure with no cuts except normal-threshold cuts. Moreover, in the Bergman-Weil representation of the asymptotic amplitude the generalized Steinmann relations can be imposed, since all of the bad boundaries are inaccessible, and hence can be defined to be the corresponding M^G.

Finally, the different terms in the Bergman-Weil representation can be grouped together into components, each of which corresponds to a hexagraph $\tilde{H}$, and which has only those singularities indicated by the flow graphs that correspond to this hexagraph.

Note that the function $\tilde{H}(C)$ maps the tree diagram $\tau(C)$ corresponding to the set of $(n-3)$ uncrossed direct channel cuts C onto a hexagraph. This hexagraph, when read sideways, represents a specific set of $n-3$ uncrossed cuts in a specific crossed channel. Thus the function $\tilde{H}(C)$ maps a tree diagram $\tau(C)$ representing a particular set of $n-3$ direct channel cuts into tree diagrams representing a particular set of $n-3$ cross channel cuts. This connection between direct channel trees and cross channel trees, taken in conjunction with the Bergman-Weil decomposition into hexagraphical components is the basis of White's analysis.

REFERENCE

(1) N. Bali, G. F. Chew, and A. Pignotti, Phys. Rev. 163 (1967) 1572.

(2) C. Fronsdal, R. E. Norton, and K. T. Mahanthappa, Phys. 127 (1962) 1848; J. Math Phys. 4 (1963) 859.

(3) B. A. Fuks, Introduction to the Theory of Analytic Functions of Several Complex Variables (Amer. Math. Soc., Providence, Rhode Island, 1963).

(4) H. P. Stapp and J. L. Wright, Nuovo Cimento 57A (1968) 475.

0 0 0 0 4 5 0 1 9 3 6

LEGAL NOTICE

This report was prepared as an account of work sponsored by the United States Government. Neither the United States nor the United States Energy Research and Development Administration, nor any of their employees, nor any of their contractors, subcontractors, or their employees, makes any warranty, express or implied, or assumes any legal liability or responsibility for the accuracy, completeness or usefulness of any information, apparatus, product or process disclosed, or represents that its use would not infringe privately owned rights.

TECHNICAL INFORMATION DIVISION
LAWRENCE BERKELEY LABORATORY
UNIVERSITY OF CALIFORNIA
BERKELEY, CALIFORNIA 94720